28 March 2000

A study of the $\eta\eta$ channel produced in central pp interactions at 450 GeV/c

The WA102 Collaboration

D. Barberis[4], F.G. Binon[6], F.E. Close[3,4], K.M. Danielsen[11], S.V. Donskov[5], B.C. Earl[3], D. Evans[3], B.R. French[4], T. Hino[12], S. Inaba[8], A. Jacholkowski[4], T. Jacobsen[11], G.V. Khaustov[5], J.B. Kinson[3], A. Kirk[3], A.A. Kondashov[5], A.A. Lednev[5], V. Lenti[4], I. Minashvili[7], J.P. Peigneux[1], V. Romanovsky[7], N. Russakovich[7], A. Semenov[7], P.M. Shagin[5], H. Shimizu[10], A.V. Singovsky[1,5], A. Sobol[5], M. Stassinaki[2], J.P. Stroot[6], K. Takamatsu[9], T. Tsuru[8], O. Villalobos Baillie[3], M.F. Votruba[3], Y. Yasu[8].

Abstract

The reaction $pp \rightarrow p_f(\eta\eta)p_s$ has been studied at 450 GeV/c. For the first time a partial wave analysis of the centrally produced $\eta\eta$ system has been performed. Signals for the $f_0(1500)$, $f_0(1710)$ and $f_2(2150)$ are observed and the decay branching fractions of these states are determined.

Submitted to Physics Letters

[1] LAPP-IN2P3, Annecy, France.
[2] Athens University, Physics Department, Athens, Greece.
[3] School of Physics and Astronomy, University of Birmingham, Birmingham, U.K.
[4] CERN - European Organization for Nuclear Research, Geneva, Switzerland.
[5] IHEP, Protvino, Russia.
[6] IISN, Belgium.
[7] JINR, Dubna, Russia.
[8] High Energy Accelerator Research Organization (KEK), Tsukuba, Ibaraki 305-0801, Japan.
[9] Faculty of Engineering, Miyazaki University, Miyazaki 889-2192, Japan.
[10] RCNP, Osaka University, Ibaraki, Osaka 567-0047, Japan.
[11] Oslo University, Oslo, Norway.
[12] Faculty of Science, Tohoku University, Aoba-ku, Sendai 980-8577, Japan.

The $\eta\eta$, $\eta\eta'$ and $\eta'\eta'$ channels are important for the determination of the gluonic content of mesons, since it is thought likely that glueballs will decay with the emission of ηs and η's [1, 2]. In addition, central production is proposed as a good place to produce glueballs via Double Pomeron Exchange (DPE) [2, 3]. Hence the interest of the present paper which studies the centrally produced $\eta\eta$ system.

The $\eta\eta$ channel has been studied previously in radiative J/ψ decays by the Crystal Ball experiment [4], in π^-p interactions by the NA12 experiment [5, 6], in central production by NA12/2 [7] and in $p\overline{p}$ annihilations by the Crystal Barrel Collaboration [8] and E760 at Fermilab [9]. In all these reactions evidence for the $f_0(1500)$ has emerged. In addition, in $p\overline{p}$ annihilation evidence is claimed for a $f_0(2100)$ [9, 10] and an $\eta\eta$ decay mode of the $f_2(1950)$ [10]. In π^-p interactions the NA12 experiment claim a $f_0(2000)$ [6]. In radiative J/ψ decays evidence was reported for the $f_J(1710)$ [4]. In central production the NA12/2 experiment claimed evidence for a $f_2(2175)$ [7].

In this paper a study is presented of the $\eta\eta$ final state formed in the reaction

$$pp \rightarrow p_f(\eta\eta)p_s \tag{1}$$

at 450 GeV/c. It represents more than a factor of 6 increase in statistics over the only other data on the centrally produced $\eta\eta$ final state [7] and moreover will present the first partial wave analysis of this channel in central production. The data come from the WA102 experiment which has been performed using the CERN Omega Spectrometer, the layout of which is described in ref. [11]. Reaction (1) has been isolated using the following decay modes:

$$\begin{array}{rr} \eta \rightarrow \gamma\gamma & \eta \rightarrow \gamma\gamma \\ \eta \rightarrow \gamma\gamma & \eta \rightarrow \pi^+\pi^-\pi^0 \\ \eta \rightarrow \pi^+\pi^-\pi^0 & \eta \rightarrow \pi^+\pi^-\pi^0 \end{array}$$

The above decay modes account for 38.8 % of the total.

Fig. 1a) shows a scatter plot of $M(\gamma\gamma)$ versus $M(\gamma\gamma)$ which has been extracted from the sample of events having two outgoing charged tracks and four γs reconstructed in the GAMS-4000 calorimeter using momentum and energy balance. A clear signal of the $\eta\eta$ channel can be observed. Fig. 1b) shows the $\gamma\gamma$ mass spectrum if the other $\gamma\gamma$ pair is compatible with being an η (0.48 $\leq$ M($\gamma\gamma$) $\leq$ 0.62 GeV) where a clear η signal can be observed. The $\eta\eta$ final state has been selected using the mass cuts described above.

Fig. 1c) shows a scatter plot of $M(\gamma\gamma)$ versus M($\pi^+\pi^-\pi^0$) for the sample of events having four outgoing charged tracks and four γs reconstructed in the GAMS-4000 calorimeter after imposing momentum and energy balance. A clear signal of the $\eta\eta$ channel can be observed. Fig. 1d) shows the $\pi^+\pi^-\pi^0$ mass spectrum if the $\gamma\gamma$ mass is compatible with being an η (0.48 $\leq$ M($\gamma\gamma$) $\leq$ 0.62 GeV) and fig 1e) shows the $\gamma\gamma$ mass spectrum if the $\pi^+\pi^-\pi^0$ mass is compatible with being an η (0.52 $\leq$ M($\pi^+\pi^-\pi^0$) $\leq$ 0.58 GeV). The $\eta\eta$ final state has been selected by requiring that 0.48 $\leq$ M($\gamma\gamma$) $\leq$ 0.62 GeV and 0.52 $\leq$ M($\pi^+\pi^-\pi^0$) $\leq$ 0.58 GeV.

Fig. 1f) shows a scatter plot of $M(\pi^+\pi^-\pi^0)$ versus $M(\pi^+\pi^-\pi^0)$ for the the sample of events having six outgoing charged tracks and four γs reconstructed in the GAMS-4000 calorimeter after imposing momentum and energy balance. A signal of the $\eta\eta$ channel can be observed.

Fig. 1g) shows the $\pi^+\pi^-\pi^0$ mass spectrum if the other $\pi^+\pi^-\pi^0$ combination has a mass compatible with being an η ($0.52 \leq$ M($\pi^+\pi^-\pi^0$) ≤ 0.58 GeV). The $\eta\eta$ final state has been selected using the mass cuts described above.

The background below the η signal has several sources including combinatorics, fake gammas and other channels. The combinatorial background is removed, in part, in the selection procedure. The remaining background varies from 16 % to 32 % dependent on the decay topology. Three methods have been used to determine the effects of this background; studying the side bands around the η signal, studying events that do not balance momentum and using event mixing. All three methods give a similar background which peaks near threshold in the $\eta\eta$ mass spectrum. To illustrate this point, superimposed on figs. 1b), d), e) and g) as a shaded histogram are the respective mass distributions when the central system has a mass greater than 1.3 GeV. As can be seen the background below the η signal is reduced with respect to the total sample. In the remainder of this paper the method used to determine the background will be the one using events that do not balance momentum. The resulting distributions well represent the background in the data.

The $\eta\eta$ mass spectra from each decay mode are very similar and the combined mass spectrum is shown in fig. 2a) and consists of 3351 events. Superimposed on the mass spectrum as a shaded histogram is the estimate of the background. Fig. 2b) shows the background subtracted mass spectrum. The mass spectrum has a threshold enhancement and has peaks at 1.5 and 2.1 GeV and a shoulder in the 1.7 GeV region. Superimposed on fig 2b) as a shaded histogram is the expected contribution from the $f_2(1270)$ (47 events) and $f_2'(1525)$ (3 events) using the observed $f_2(1270)$ signal in the $\pi^+\pi^-$ final state [12], the observed $f_2'(1525)$ signal in the K^+K^- final state [13] and correcting for the experimental acceptance and using the PDG [14] branching ratios. As can be seen the majority of the signal at 1.5 GeV is not due to the $f_2'(1525)$.

A Partial Wave Analysis (PWA) of the centrally produced $\eta\eta$ system has been performed assuming the $\eta\eta$ system is produced by the collision of two particles (referred to as exchanged particles) emitted by the scattered protons. The z axis is defined by the momentum vector of the exchanged particle with the greatest four-momentum transferred in the $\eta\eta$ centre of mass. The y axis is defined by the cross product of the momentum vectors of the two exchanged particles in the pp centre of mass. The two variables needed to specify the decay process were taken as the polar and azimuthal angles (θ, ϕ) of one of the ηs in the $\eta\eta$ centre of mass relative to the coordinate system described above.

The acceptance corrected moments $\sqrt{4\pi}t_{LM}$, defined by

$$I(\Omega) = \sum_L t_{L0} Y_L^0(\Omega) + 2 \sum_{L,M>0} t_{LM} Re\{Y_L^M(\Omega)\}$$

have been rescaled to the total number of observed events and are shown in fig. 3. The moments with $M > 2$ and all the moments with $L > 4$ (e.g. the t_{44} and t_{60} moments shown in fig. 3) are small and hence only partial waves with spin $l = 0$ and 2 and absolute values of spin z-projection $m \leq 1$ have been included in the PWA.

The amplitudes used for the PWA are defined in the reflectivity basis [15]. In this basis the angular distribution is given by a sum of two non-interfering terms corresponding to negative and positive values of reflectivity. The waves used were of the form J^{ε}_{m} with $J = S$ and D, $m = 0, 1$ and reflectivity $\varepsilon = \pm 1$. The expressions relating the moments (t_{LM}) and the waves (J^{ε}_{m}) are given in ref.[16]. Since the overall phase for each reflectivity is indeterminate, one wave in each reflectivity can be set to be real (S^{-}_{0} and D^{+}_{1} for example) and hence two phases can be set to zero ($\phi_{S^{-}_{0}}$ and $\phi_{D^{+}_{1}}$ have been chosen). This results in 6 parameters to be determined from the fit to the angular distributions.

The PWA has been performed independently in 80 MeV intervals of the $\eta\eta$ mass spectrum. In each mass an event-by-event maximum likelihood method has been used. The function

$$F = -\sum_{i=1}^{N} ln\{I(\Omega)\} + \sum_{L,M} t_{LM}\epsilon_{LM} \quad (2)$$

has been minimised, where N is the number of events in a given mass bin, ϵ_{LM} are the efficiency corrections calculated in the centre of the bin and t_{LM} are the moments of the angular distribution. The moments calculated from the partial amplitudes are shown superimposed as histograms on the experimental moments in fig 3. As can be seen the results of the fit reproduce well the experimental moments.

The system of equations which express the moments via the partial wave amplitudes is non-linear which leads to inherent ambiguities. For a system with S and D waves there are two solutions for each mass bin. In each mass bin one of these solutions is found from the fit to the experimental angular distributions, the other one can then be calculated by the method described in ref. [15]. In the case under study the bootstrapping procedure is trivial because the Barrelet function has only two roots (Z_i with i = 1,2) and their real and imaginary parts do not cross zero as functions of mass, as seen in fig 2c) and d). In order to link the solutions in adjacent mass bins, the real parts of the roots are sorted in each mass bin in such a way that the real part of the first root should be larger than the real part of the second root (real parts of the two roots have different signs). For the first solution the imaginary parts of both roots are taken positive, the second solution is obtained by complex conjugation of one of the roots.

In this case two different PWA solutions are found. One solution is dominated by the S-wave the other solution has the events split between the different D-waves. By definition both solutions give identical moments and identical values of the likelihood. A Monte Carlo study has shown that if the input distribution is really dominated by a D-wave (i.e. D^{-}_{0}, D^{-}_{1} or D^{+}_{1}) then both solutions of the PWA will be dominated by that D-wave. However, if the input distribution is dominated by the S-wave then two different solutions will result. One of the PWA solutions will be dominated by the S-wave, the other solution will be split equally between the D-waves and hence the physical solution can still be determined. The physical solution is shown in fig. 4. The S^{-}_{0}-wave for the physical solution is characterised by a broad enhancement at threshold and a peak at 1.5 GeV. A broad enhancement is also seen in the D^{-}_{0}-wave at 2.1 GeV. Superimposed on the waves as a histogram is the result of running the PWA on the background events.

Fig. 5 shows the background subtracted S^{-}_{0} and D^{-}_{0} waves. The PWA analysis has also been performed by extending the likelihood function given in equation (2) to include the background subtraction, namely

$$F = -\sum_{i=1}^{N} ln\{I(\Omega)\} + \sum_{L,M} t_{LM}\epsilon_{LM} + \sum_{i=1}^{N_{bg}} ln\{I(\Omega)\}$$

where N_{bg} is the number of background events. Since the background is dominantly S-wave the results of this method are similar to those shown in fig. 5.

The S_0^--wave has been fitted using a K-matrix parameterisation similar to that used to fit the K^+K^- spectrum [17] with the addition of an incoherent background term. Poles have been introduced to describe the $f_0(1370)$, $f_0(1500)$ and $f_0(1710)$ with parameters fixed to those found from the coupled channel fit to the $\pi^+\pi^-$ and K^+K^- spectra [17], namely M($f_0(1370)$) = 1312 MeV, $\Gamma(f_0(1370))$ = 218 MeV, M($f_0(1500)$) = 1502 MeV, $\Gamma(f_0(1500))$ = 98 MeV and M($f_0(1710)$) = 1727 MeV, $\Gamma(f_0(1710))$ = 126 MeV. The fit describes well the data but, due to the size of the errors, it is not possible to conclude about the need for a further resonance above 2 GeV. The inclusion of the $f_0(1710)$ is essential to describe the spectrum.

The D_0^- wave has been fitted using two spin 2 relativistic Breit-Wigners and a linear background. The first Breit-Wigner is used to describe the $f_2(1270)$ with mass and width fixed to the PDG values [14] and the second to describe the peak at 2.1 GeV where we have used M = 2130 MeV, Γ = 270 MeV which are the parameters found for $f_2(2150)$ observed in the K^+K^- final state [13]. As can be seen the fit well describes the data. This state is compatible with the $f_2(2175)$ previously observed by the NA12/2 experiment in the $\eta\eta$ final state [7].

The error bars introduced by the partial wave analysis do not allow the parameters of the resonances to be determined from a free fit to the waves. Instead, we have performed a fit to the total mass spectrum shown in fig. 2b) using an incoherent sum of the expressions used to fit the S_0^- and D_0^- waves. The parameters for the $f_0(1370)$ and $f_2(1270)$ have been fixed to the values used above. The fit is shown superimposed on fig. 2b) and for the scalar resonances yields sheet II T-Matrix poles [18] at

$$\begin{array}{llll} f_0(1500) & \mathrm{M} & = (1510 \pm 8) \; -i\,(55 \pm 8) & \mathrm{MeV} \\ f_0(1710) & \mathrm{M} & = (1698 \pm 18) \; -i\,(60 \pm 13) & \mathrm{MeV} \end{array}$$

These parameters are consistent with the PDG [14] values for these resonances and our previous fits [17]. For the $f_2(2150)$ the fit gives

$$f_2(2150) \qquad \mathrm{M} = 2151 \pm 16 \ \mathrm{MeV}, \qquad \Gamma = 280 \pm 70 \ \mathrm{MeV}.$$

The parameters found are compatible with those from the K^+K^- channel [13].

After correcting for the unseen decay modes and using data from the previously observed $\pi\pi$ [12, 16] final state the branching ratio $\eta\eta\ /\pi\pi$ has been calculated for the $f_0(1500)$ from the fit to the S_0^- wave and gives :

$$\frac{f_0(1500) \to \eta\eta}{f_0(1500) \to \pi\pi} = 0.18 \pm 0.03$$

This value agrees well with the value that can be derived from the PDG [14] of 0.23 $\pm$ 0.10.

For the $f_2(1270)$ the ratio is

$$\frac{f_2(1270) \to \eta\eta}{f_2(1270) \to \pi\pi} = (3 \pm 1) \times 10^{-3}$$

which is compatible with the PDG [14] value.

For the $f_0(1500)$, $f_0(1710)$ and $f_2(2150)$ the branching ratio $\eta\eta\ /K\overline{K}$ has been calculated from the WA102 data to be:

$$\frac{f_0(1500) \to \eta\eta}{f_0(1500) \to K\overline{K}} = 0.54 \pm 0.12$$

$$\frac{f_0(1710) \to \eta\eta}{f_0(1710) \to K\overline{K}} = 0.48 \pm 0.15$$

$$\frac{f_2(2150) \to \eta\eta}{f_2(2150) \to K\overline{K}} = 0.78 \pm 0.14$$

The branching ratios for the $f_0(1500)$, $f_0(1710)$ and $f_2(2150)$ differ from that of a known $s\overline{s}$ state, the $f_2'(1525)$, which has a ratio of 0.12 $\pm$ 0.04 [14] which is consistent with the SU(3) prediction for such a state [19]. No signal is seen for the $f_2'(1525)$ in the $\eta\eta$ final state of WA102 and an upper limit for its decay to this channel has been calculated, which gives

$$\frac{f_2'(1525) \to \eta\eta}{f_2'(1525) \to K\overline{K}} < 0.14 \ \ (90\% \ \ CL)$$

which is compatible with the PDG [14] value given above.

For the $f_0(1370)$ there is considerable uncertainty due to the background subtraction which mainly affects the S_0^- wave at threshold. The strongest $f_0(1370)$ signal has been observed in the 4π final state therefore the branching ratio $\eta\eta\ /4\pi$ has been calculated to be

$$\frac{f_0(1370) \to \eta\eta}{f_0(1370) \to 4\pi} = (4.7 \pm 2) \times 10^{-3}$$

which is compatible with the Crystal Barrel measurement of (1.7 $\pm$ 0.9)$\times10^{-3}$ [20].

In the D-waves there is no evidence for the $f_2(1950)$ which has been claimed to have been seen in the $\eta\eta$ final states formed in $p\overline{p}$ annihilations [10]. Since the $f_2(1950)$ is clearly seen in the 4π final state of experiment WA102 [21], an upper limit for its decay to $\eta\eta$ has been calculated and gives

$$\frac{f_2(1950) \to \eta\eta}{f_2(1950) \to 4\pi} < 5.0 \times 10^{-3} \ \ (90\% \ \ CL)$$

Hence this would imply that if the observation in the $\eta\eta$ final state of $p\overline{p}$ annihilations is correct, then a very large signal for the $f_2(1950)$ should be seen in the 4π final state of the same experiment.

The $f_0(1500)$ has previously been observed in the $\pi\pi$ [12, 16], $K\overline{K}$ [13], 4π [21] and $\eta\eta'$ [22] final states of the WA102 experiment. The relative decay rates for the $f_0(1500)$ are calculated to be:

$$\pi\pi : K\overline{K} : \eta\eta : \eta\eta' : 4\pi = 1 \ : \ 0.33 \pm 0.07 \ : \ 0.18 \pm 0.03 \ : \ 0.096 \pm 0.026 \ : \ 1.36 \pm 0.15$$

The $f_0(1370)$ is below $\eta\eta'$ threshold. The remaining relative decay rates for the $f_0(1370)$ are:

$$\pi\pi : K\overline{K} : \eta\eta : 4\pi = 1 : 0.46 \pm 0.19 : 0.16 \pm 0.07 : 34.0^{+22}_{-9}$$

No signal was observed for the $f_0(1710)$ in the 4π [21] or the $\eta\eta'$ channels [22]. Therefore, an upper limit has been calculated for its decay to these final states. For the $f_0(1710)$ the relative decay rates are:

$$\pi\pi : K\overline{K} : \eta\eta : \eta\eta' : 4\pi = 1 : 5.0 \pm 0.7 : 2.4 \pm 0.6 :< \ 0.18 \ (90\ \% \ \ CL) :< \ 5.4 \ (90\ \% \ \ CL)$$

In summary, a partial wave analysis of the $\eta\eta$ channel has been performed for the first time in central production. Clear evidence is found for an $\eta\eta$ decay mode of the $f_0(1500)$, $f_0(1710)$ and $f_2(2150)$ and the decay branching ratios of these states have been determined.

Acknowledgements

This work is supported, in part, by grants from the British Particle Physics and Astronomy Research Council, the British Royal Society, the Ministry of Education, Science, Sports and Culture of Japan (grants no. 07044098 and 1004100), the French Programme International de Cooperation Scientifique (grant no. 576) and the Russian Foundation for Basic Research (grants 96-15-96633 and 98-02-22032).

References

[1] S. S. Gershtein *et al.,* Zeit. Phys. **C24** (1984) 305;
R. Akhoury and J.M. Frere, Phys. Lett. **B220** (1989) 258.

[2] F. E. Close, Rep. Prog. Phys. **51** (1988) 833.

[3] D. Robson *et al.,* Nucl. Phys. **B130** (1977) 328.

[4] C. Edwards *et al.,* Phys. Rev. Lett. **48** (1982) 458.

[5] F. Binon *et al.,* Il Nuovo Cimento **A78** (1983) 313.

[6] A.A. Kondashov *et al.,* Frascati Physics Series **XV** (1999) 257.

[7] D. Alde *et al.,* Phys. Lett. **B201** (1988) 160;
A. Singovski, Il Nuovo Cimento **A107** (1993) 1911.

[8] C. Amsler *et al.,* Phys. Lett. **B353** (1995) 571;
A. Abele *et al.,* Euro Physics Journal **C 8** (1999) 67.

[9] T.A. Armstrong *et al.,* Phys. Lett. **B307** (1993) 394.

[10] A.V. Anisovich *et al.,* Phys. Lett. **B449** (1999) 145.

[11] D. Barberis *et al.,* Phys. Lett. **B397** (1997) 339.

[12] D. Barberis *et al.,* Phys. Lett. **B453** (1999) 316.

[13] D. Barberis *et al.,* Phys. Lett. **B453** (1999) 305.

[14] Particle Data Group, European Physical Journal **C3** (1998) 1.

[15] S.U. Chung, Phys. Rev. **D56** (1997) 7299.

[16] D. Barberis *et al.,* Phys. Lett. **B453** (1999) 325.

[17] D. Barberis *et al.,* Phys. Lett. **B462** (1999) 462.

[18] D. Morgan, Phys. Lett. **B51** (1974) 71.

[19] Yu. Prokoshkin, Proceedings of Hadron 91, Maryland, USA 1991;
Yu. Prokoshkin, Sov. Phys. Dokl. **316** (1991) 155;
S. Godfrey and N. Isgur, Phys. Rev. **D261** (1985) 189.

[20] U. Thoma, Proceedings of Hadron 99, Beijing, China 1999.

[21] S. Abatzis *et al.,* Phys. Lett. **B324** (1994) 509;
D. Barberis *et al.,* Phys. Lett. **B413** (1997) 217;
D. Barberis *et al.,* Phys. Lett. **B471** (2000) 440;
D. Barberis *et al.,* Phys. Lett. **B474** (2000) 423.

[22] D. Barberis *et al.,* Phys. Lett. **B471** (2000) 429.

Figures

Figure 1: Selection of the $\eta\eta$ final state. For the reaction $pp \to p_f p_s(4\gamma)$ a) M($\gamma\gamma$) versus M($\gamma\gamma$) and b) M($\gamma\gamma$) if the other $\gamma\gamma$ pair is in the η band ($0.48 \leq$ M($\gamma\gamma$) ≤ 0.62 GeV). For the reaction $pp \to p_f p_s(\pi^+\pi^-\pi^0 2\gamma)$ c) M($\gamma\gamma$) versus M($\pi^+\pi^-\pi^0$), d) M($\pi^+\pi^-\pi^0$) if the $\gamma\gamma$ mass is in the η band ($0.48 \leq$ M($\gamma\gamma$) ≤ 0.62 GeV) and e) M($\gamma\gamma$) if the $\pi^+\pi^-\pi^0$ mass is in the η band ($0.52 \leq$ M($\pi^+\pi^-\pi^0$) ≤ 0.58 GeV). For the reaction $pp \to p_f p_s(\pi^+\pi^-\pi^+\pi^-\pi^0\pi^0)$ f) $M(\pi^+\pi^-\pi^0)$ versus M($\pi^+\pi^-\pi^0$) and g) M($\pi^+\pi^-\pi^0$) if the other $\pi^+\pi^-\pi^0$ mass is in the η band ($0.52 \leq$ M($\pi^+\pi^-\pi^0$) ≤ 0.58 GeV). Superimposed as a shaded histogram are the respective histograms when the central system has a mass greater then 1.3 GeV.

Figure 2: a) The $\eta\eta$ mass spectrum. Superimposed as a shaded histogram is an estimation of the background contribution. b) The background subtracted $\eta\eta$ mass spectrum with fit described in the text. Superimposed as a shaded histogram is an estimation of the $f_2(1270)$ and $f_2'(1525)$ contribution. The c) Real and d) Imaginary parts of the roots (Z, see text) as a function of mass obtained from the PWA of the $\eta\eta$ system.

Figure 3: The $\sqrt{4\pi}t_{LM}$ moments from the data. Superimposed as a solid histogram are the resulting moments calculated from the PWA of the $\eta\eta$ final state.

Figure 4: The physical solution from the PWA of the $\eta\eta$ final state. Superimposed as a shaded histogram is an estimation of the background contribution.

Figure 5: The background subtracted a) S_0^- and b) D_0^- waves with fits described in the text. The parameters used to describe the resonances are those previously determine from the $\pi\pi$ and $K\overline{K}$ channels.

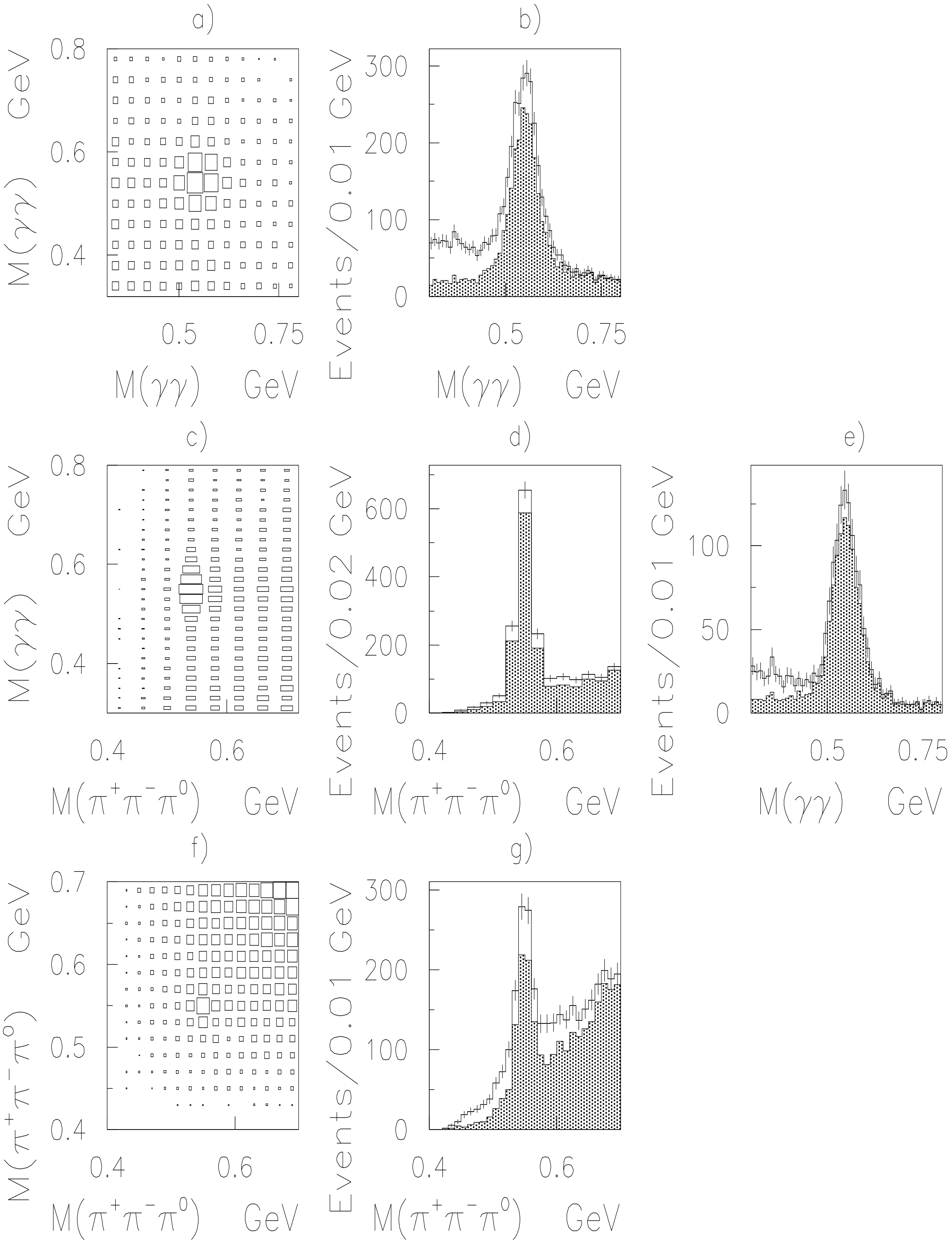
a)
0.8
0.6
0.4
M(γγ) GeV
0.5
0.75
M(γγ) GeV
b)
300
200
100
0
Events/0.01 GeV
0.5
0.75
M(γγ) GeV
c)
0.8
0.6
0.4
M(γγ) GeV
0.4
0.6
M(π+π−π0) GeV
d)
600
400
200
0
Events/0.02 GeV
0.4
0.6
M(π+π−π0) GeV
e)
100
50
0
Events/0.01 GeV
0.5
0.75
M(γγ) GeV
f)
0.7
0.6
0.5
0.4
M(π+π−π0) GeV
0.4
0.6
M(π+π−π0) GeV
g)
300
200
100
0
Events/0.01 GeV
0.4
0.6
M(π+π−π0) GeV

Figure 1

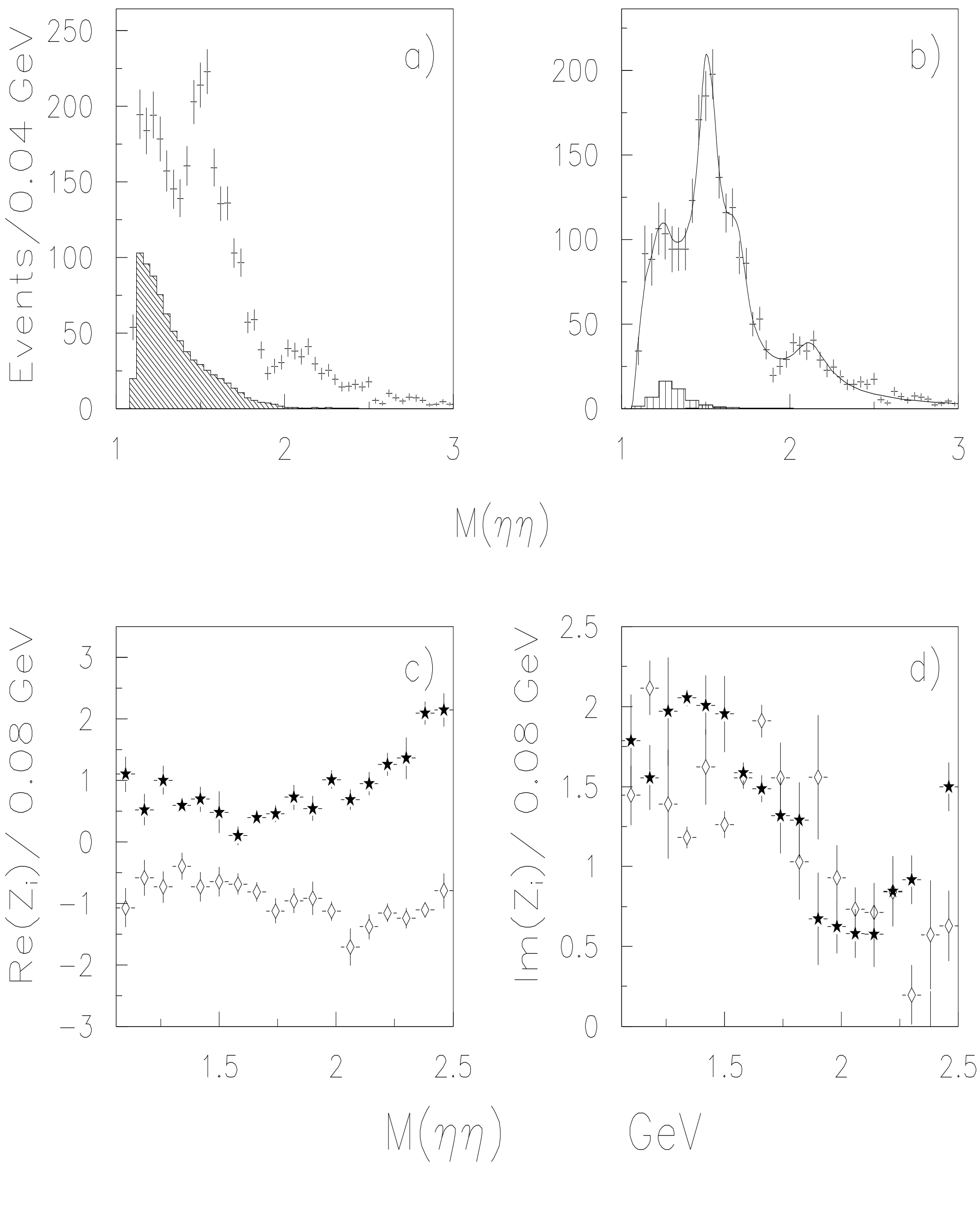

Events/0.04 GeV
250
200
150
100
50
0
a)
1
2
3
200
150
100
50
0
b)
1
2
3
M(ηη)
Re(Z_i)/ 0.08 GeV
3
2
1
0
−1
−2
−3
c)
1.5
2
2.5
Im(Z_i)/ 0.08 GeV
2.5
2
1.5
1
0.5
0
d)
1.5
2
2.5
M(ηη)
GeV

Figure 2

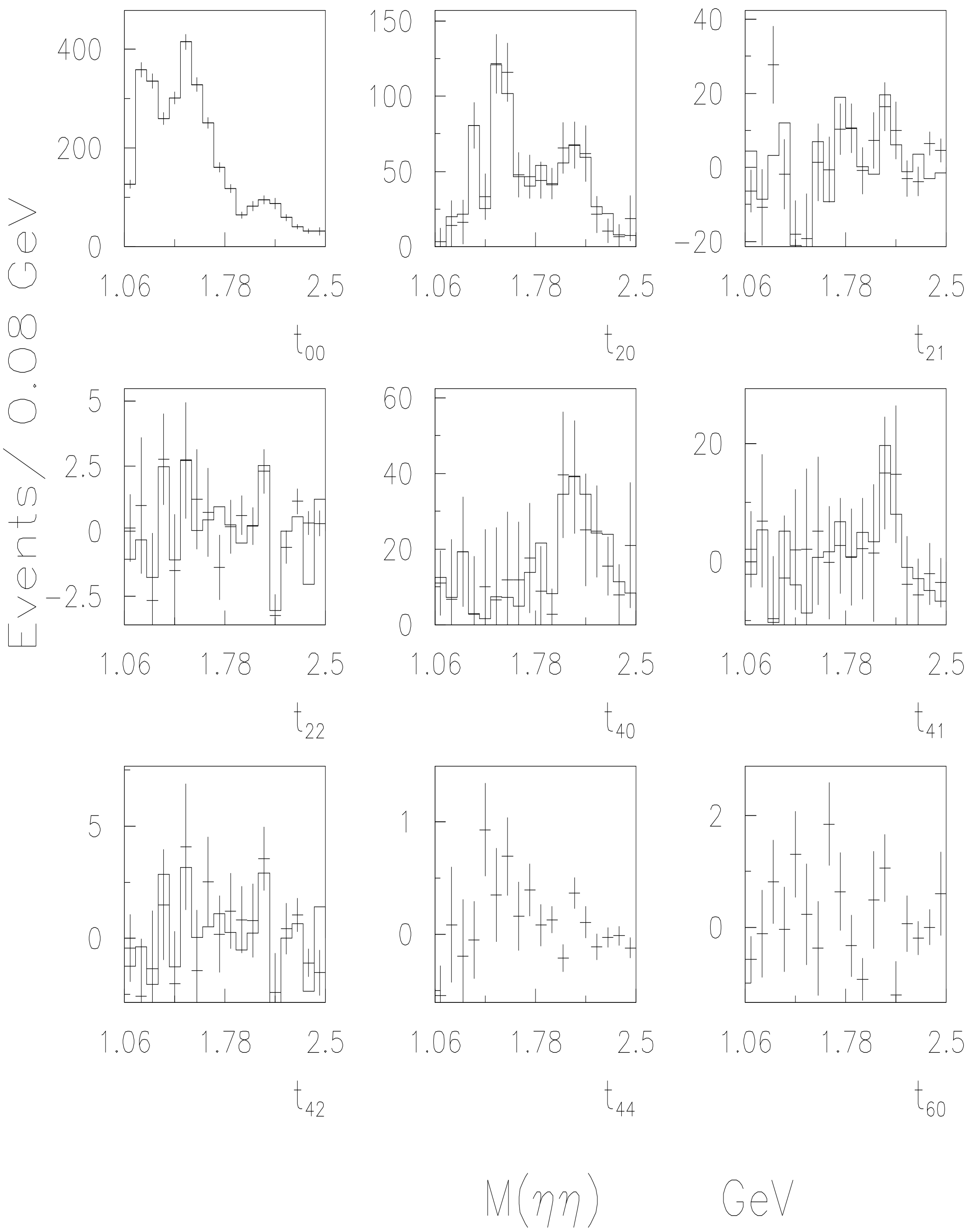
Events/ 0.08 GeV
400
200
0
1.06
1.78
2.5
t_{00}
150
100
50
t_{20}
40
20
−20
t_{21}
5
2.5
−2.5
t_{22}
60
t_{40}
t_{41}
t_{42}
1
t_{44}
2
t_{60}
M($\eta\eta$) GeV

Figure 3

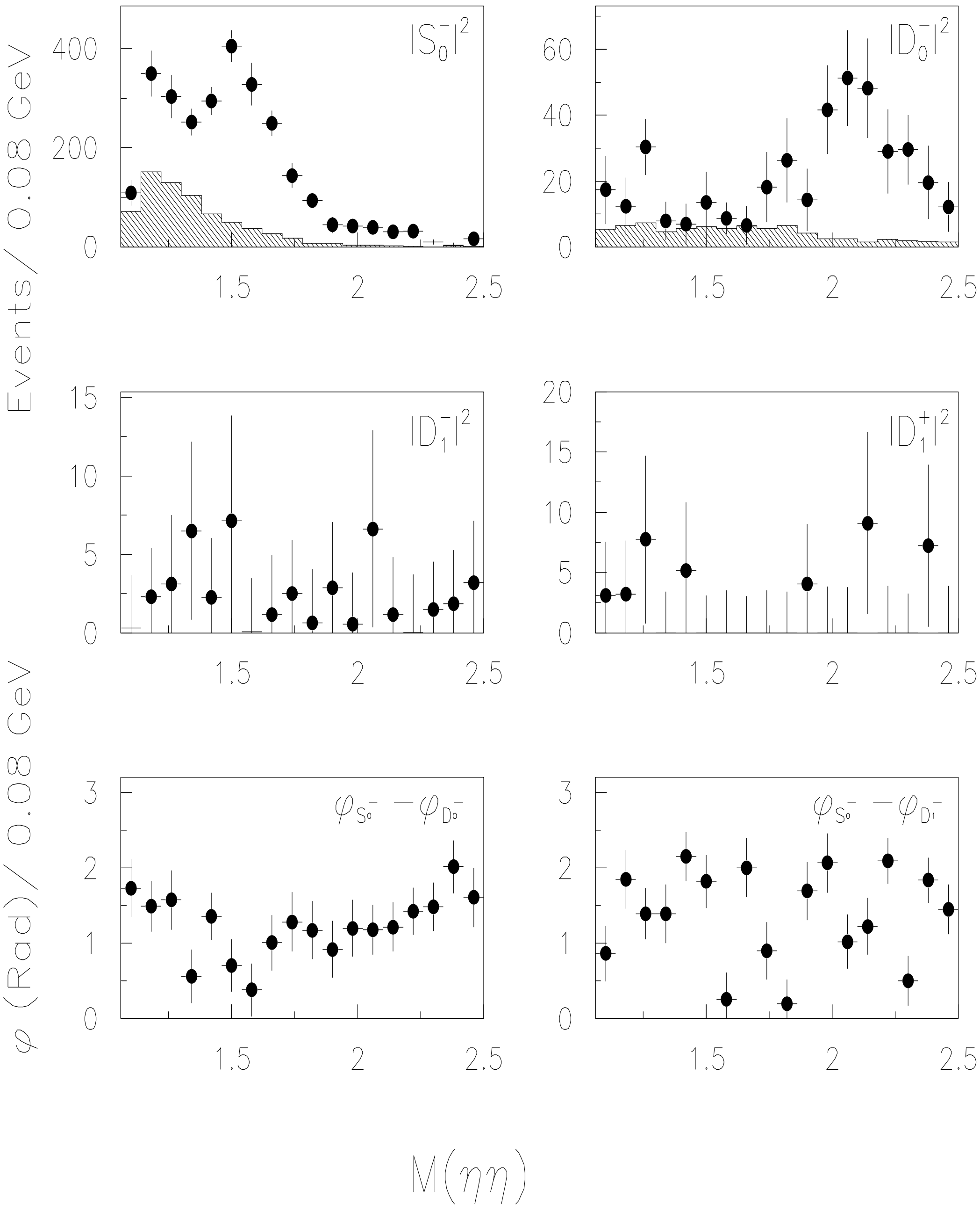

Events/ 0.08 GeV
$|S_0^-|^2$
$|D_0^-|^2$
$|D_1^-|^2$
$|D_1^+|^2$
φ (Rad)/ 0.08 GeV
$\varphi_{S_0^-} - \varphi_{D_0^-}$
$\varphi_{S_0^-} - \varphi_{D_1^-}$
M($\eta\eta$)

Figure 4

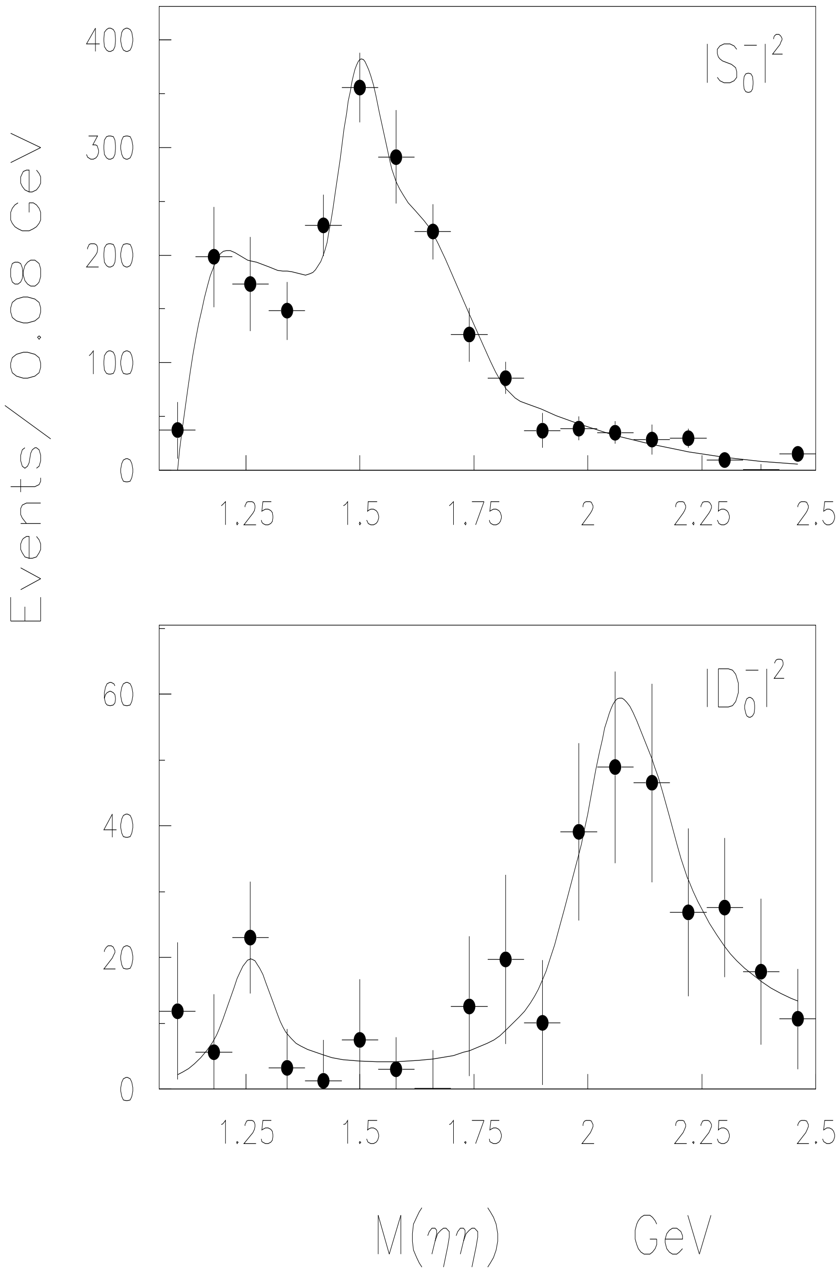

Events/ 0.08 GeV
400
300
200
100
0
$|S_0^-|^2$
1.25
1.5
1.75
2
2.25
2.5
60
40
20
0
$|D_0^-|^2$
1.25
1.5
1.75
2
2.25
2.5
M($\eta\eta$) GeV

Figure 5